JOURNAL OF BACTERIOLOGY, Oct. 2003, p. 6199–6204 Vol. 185, No. 20
0021-9193/03/$08.00+0 DOI: 10.1128/JB.185.20.6199–6204.2003

Reduced Water Availability Influences the Dynamics, Development, and Ultrastructural Properties of *Pseudomonas putida* Biofilms

Woo-Suk Chang[1] and Larry J. Halverson[1,2]*

Department of Agronomy[2] and Graduate Program in Microbiology,[1] Iowa State University, Ames, Iowa 50011-1010

Received 14 April 2003/Accepted 19 July 2003

***Pseudomonas putida* strain mt-2 unsaturated biofilm formation proceeds through three distinct developmental phases, culminating in the formation of a microcolony. The form and severity of reduced water availability alter cell morphology, which influences microcolony size and ultrastructure. The dehydration (matric stress) treatments resulted in biofilms comprised of smaller cells, but they were taller and more porous and had a thicker extracellular polysaccharide layer at the air interface. In the solute stress treatments, cell filamentation occurred more frequently in the presence of high concentrations of ionic (but not nonionic) solutes, and these filamented cells drastically altered the biofilm architecture.**

In terrestrial habitats, bacteria reside on soil matrices or plant surfaces as aggregates of cells, or microcolonies, that are frequently enmeshed in exopolymeric substances of their own making and can be described as biofilms (1, 5, 19, 23). These biofilms are commonly unsaturated, although water films, which vary in thickness depending on the environmental conditions, surround them. In a saturated system, the water potential is comprised almost exclusively of the solute potential (24). However, under unsaturated conditions, water availability is influenced by both the solute and matric potentials (24). The difference between these two stresses is that with a solute stress, bacteria are bathed in water of diminished activity but that with a matric stress, bacteria are dehydrated due to low water contents and the availability of the water is reduced through its interaction with the matrix. Under normal conditions, soil bacteria experience significant matric stress (12).

In aquatic systems, channels in the biofilm act as conduits for waste removal and nutrient supply (34). Under low-shear laminar flow, *Pseudomonas aeruginosa* PAO1 biofilms consist of a monolayer of cells with mound-shaped, circular microcolonies, but under high-shear turbulent flow, PAO1 biofilms consist of filamentous streamers (8, 14, 25). The development of this complex architecture is influenced by hydrodynamics, nutrient composition, and biological properties such as quorum sensing, extracellular polysaccharide (EPS) production, and motility (8). In unsaturated habitats, the lack of laminar fluid flow dramatically influences nutrient availability patterns, metabolic-waste accumulation and disposal, and the accumulation of cell-signaling molecules and, consequently, biofilm architecture.

Atomic-force microscopy of fresh and desiccated *Pseudomonas putida* biofilms revealed that drying had little effect on physical morphology and surface properties (1). However, those studies focused on fully developed, mature biofilms that were then dried. In many ways, the growth of bacteria on agar surfaces better approximates the conditions that bacteria experience in many unsaturated habitats; they are able to acquire nutrients from the underlying matrix and from a relatively thin water film covering the biofilm. Examination of the organization of cells within colonies grown on agar surfaces has revealed the importance of cell-cell interactions and that cells within a colony assume particular organizational patterns with unique gene expression patterns (9, 21, 27–30).

The purpose of the study reported here was to characterize the effect of reduced water availability on the development and ultrastructural properties of unsaturated *P. putida* mt-2 biofilms. We monitored biofilm development under static conditions in real time using an experimental system that we developed for visualizing microcolony formation on a solid surface by confocal scanning laser microscopy (CSLM) and epifluorescence microscopy. In order to visualize unsaturated biofilms, we tagged *P. putida* mt-2 with the green fluorescent protein by transferring a stable, broad-host-range plasmid pPROBE-KT (18) containing the *gfp* gene fused to the constitutive neomycin-phosphotransferase (P_{nptII}) promoter. We used a permeating solute (NaCl, KCl, sucrose, polyethylene glycol 200 [PEG 200; i.e., a PEG with a molecular weight of 200]) and a nonpermeating solute (PEG 8000) to simulate the solute and matric components of the soil water potential, respectively, as described previously (11, 12). Bacteria were cultivated on 50%-strength Luria-Bertani solid medium without NaCl and amended with (per liter) 1 g of $MgSO_4 \cdot 7H_2O$, 1.38 g of KH_2PO_4, 0.2 g of calcofluor white (Sigma Chemical Co., St. Louis, Mo.), 40 ml of Hutner's mineral solution (32), and 8 g of phytagel gellan gum (Sigma Chemical Co.).

We developed a chamber system (2.5 [width] by 7.5 [length] by 0.5 [diameter] cm) composed of black Delrin plastic in which biofilms grew on a thin layer of solid medium (0.2- to 0.3-mm thick) on a coverslip placed over a reservoir (1.4 by 3.5 by 0.3 cm) filled with the appropriate medium to maintain the desired relative humidity. The coverslip was placed medium side down onto the chamber after the coverslip was inoculated with a 1-μl aliquot containing 10 to 20 cells of a diluted 24-h-old plate culture, which spread to create a 3- to 5-mm-diameter spot. The coverslip was taped to the chamber surface, inverted, and incubated at 27°C. When the 100× lens objective was used,

* Corresponding author. Mailing address: Department of Agronomy, Iowa State University, Ames, IA 50011-1010. Phone: (515) 294-0495. Fax: (515) 294-3163. E-mail: larryh@iastate.edu.

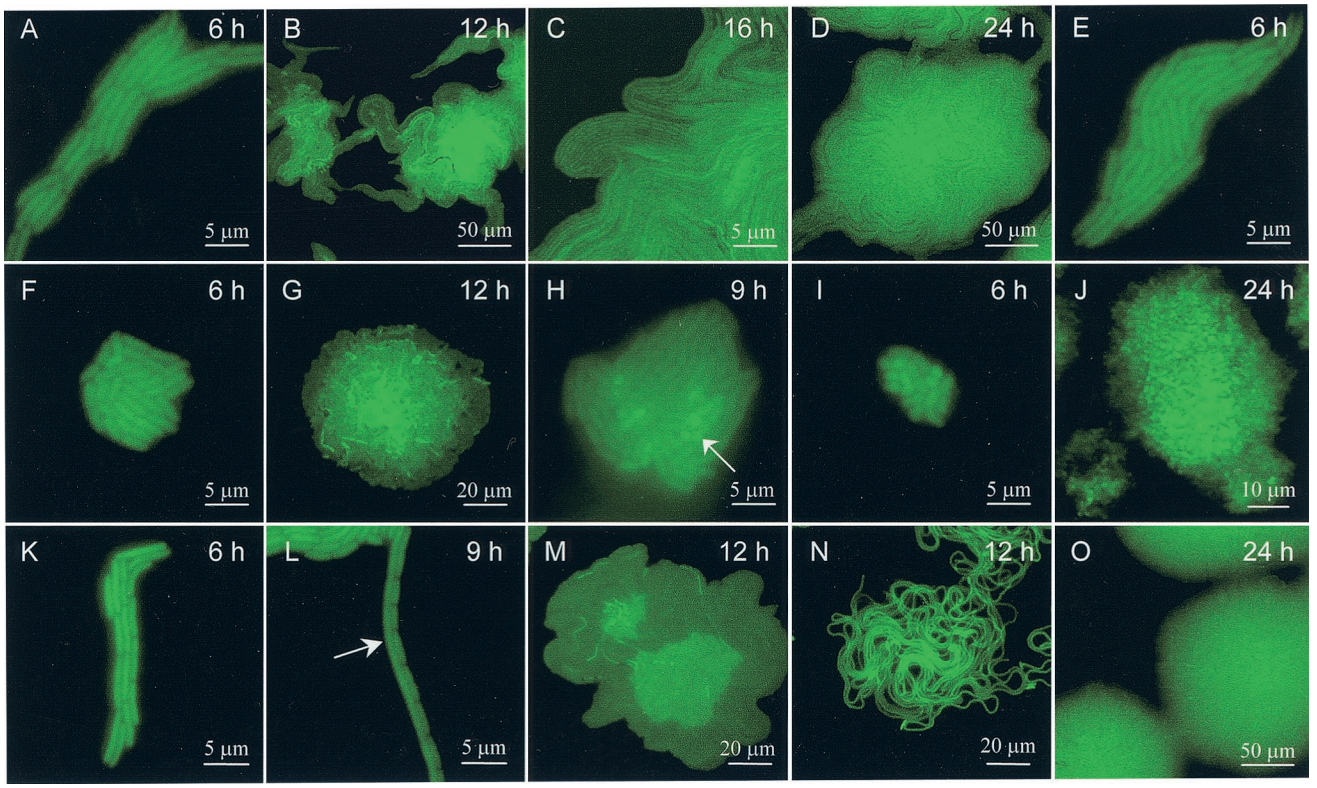

FIG. 1. Effect of reduced water availability on the temporal dynamics of *P. putida* mt-2 biofilm development. (A to D) Unamended medium; (E to J) PEG 8000-treated samples (water potentials, −0.25, −0.5, −0.5, −0.75, −1.0, and −1.5 MPa, respectively); (K to M) −0.5-MPa water potential, PEG 200-treated samples; (N to O) −1.5-MPa water potential, NaCl-treated samples. Microcolony age is indicated in the upper right-hand corner of each panel. Arrows highlight circle-shaped (H) or filamented (L) cells. We used a Nikon Instruments Inc. (Melville, N.Y.) EFD-3 epifluorescence microscope with a fluorescein isothiocyanate filter set, and images were taken with a charge-coupled device camera (SPOT camera; Diagnostic Instruments, Sterling Heights, Mich.) or a Leica TCS-NT CSLM equipped with UV and argon lasers (excitation λ = 365 and 488 nm, respectively) for visualization of calcofluor white-stained EPS (emission λ = 425 nm, short-cut filter) and green fluorescent protein (fluorescein isothiocyanate filter set) and collected by using a multitrack mode.

the coverslip was removed, inverted, and taped to a slide and then another coverslip was gently placed over the tape to cover the biofilm with minimal, if any, disturbance.

P. putida unsaturated biofilm formation proceeds in an organized fashion through early, intermediate, and maturation phases of development that are influenced by the type and severity of reduced water availability. Similar distinct developmental phases have been reported for the biofilm formation of many microorganisms in fully hydrated static and flowthrough systems (3, 7, 23), although the natures of these phases were distinct in the unsaturated biofilms studied here. Below we discuss our findings in the context of each developmental phase.

Early phase. The early phase includes an acclimation period before visible growth, and these periods were, for example, as much as 6- and 12-fold longer at water potentials of −1.0 MPa or lower in the NaCl- and PEG 8000-treated samples, respectively. Cell size changes occurring during this acclimation period were specific to the type and severity of reduced water availability, ultimately influencing biofilm development and ultrastructure. In the PEG 8000-treated samples at water potentials lower than −0.25 MPa, there were 50 to 60% reductions in cell length (Fig. 1A and E to I) that did not change with decreasing water potentials, suggesting that there was a threshold level of dehydration at which cell shrinkage occurs, possibly at an optimal surface-to-volume ratio. Cell size decreased by 25% in the PEG 200-treated biofilms (Fig. 1K to L), whereas the proportion of the cell population in a microcolony that was filamented (cells at least eight times longer than normal) increased from 3.4% ± 0.8% (mean ± standard error of the mean; number of colonies, 16 to 23) in the unamended and PEG 200-treated samples (Fig. 1L) to 66.1% ± 3.0% and 100% in the NaCl-treated samples with water potentials of −1.0- and −1.5-MPa (Fig. 1N), respectively. Filamented cells were not detected in any of the PEG 8000-treated samples at water potentials lower than −0.25 MPa. Bacterial filamentation has been observed in response to nutrient deprivation, low temperature, and high osmolarity (15, 17, 31, 33). Although the mechanism for filamentation in our study was unknown, it is possible that ionic solutes interfere with the production or action of cell division proteins involved in septation, while permitting biomass increases. Cell doubling times, as determined by monitoring the number of cells in a microcolony over the first 12 h, were 14 to 27% longer in the PEG 8000- and PEG 200-treated samples at water potentials of −1.0 MPa or lower than in the unamended samples.

Intermediate phase. The early-to-intermediate phase is comprised of the rapid growth of the rod-shaped cells parallel

TABLE 1. Influence of reduced water availability on biofilm properties[a]

Treatment and day	Microcolony surface area (μm^2)[b]	Density (cells/100 μm^2)[c]	% cell-free area[c]	Biofilm cell ht (μm)[d]	EPS thickness at air interface (μm)[e]
None					
1	32,622 ± 5,234			6.2 ± 0.3	1.5 ± 0.1
2		114.8 ± 0.8	22.2 ± 0.4	6.3 ± 0.3	1.9 ± 0.5
4	40,801 ± 2,457			6.1 ± 0.3	1.6 ± 0.1
−1.5-MPa water potential, NaCl					
1	23,899 ± 3,821			6.7 ± 0.2	2.0 ± 0.3
2		72.3 ± 0.9	24.6 ± 0.3	6.3 ± 0.2	1.9 ± 0.3
4	38,568 ± 2,457			6.8 ± 0.9	1.9 ± 0.1
−1.5-MPa water potential, PEG 8000					
1	1,568 ± 405			11.0 ± 0.8	2.7 ± 0.5
2		71.8 ± 1.6	49.7 ± 1.1	12.3 ± 0.4	3.5 ± 0.2
4	4,900 ± 1,056			14.4 ± 0.9	3.9 ± 0.5

[a] Data are expressed as means ± standard errors of the means.
[b] Microcolony area at the substratum surface. Values were derived from the average microcolony surface area per field of view (number of samples, 3 to 4) containing 1 to 14 microcolonies.
[c] The proportion of a 100-μm^2 area devoid of cells. Values were derived from 29 to 39 *x-y* plane CSLM images from 8 to 13 randomly chosen microcolonies obtained in two separate experiments.
[d] The height from the substratum to the top of biofilm. Values were derived from nine random height measurements of three to eight *x-y* projections of a stacked series of *x-y* plane CSLM images.
[e] The thickness of the calcofluor-stained layer from the top of the biofilm to the air interface. Values were derived from the images used for the biofilm cell height measurements.

to the nutrient-containing surface (Fig. 1A to C, E, F, H, I, and K to N); this orientation likely maximizes the surface area for nutrient and waste diffusion into and out of the cell. Except for the occasional presence of filamented cells, morphology was relatively constant during this phase. The type and severity of reduced water availability influenced the nature of the radial expansion of the microcolony. There was great heterogeneity in the patterns of cell alignment, and each colony harbors within it a pattern related to the biofilm developmental history initiated during this phase. On the unamended and PEG 200-treated samples, cells initially formed elongated, curved microcolonies (Fig. 1A and K), and by 12 h, the microcolony center was usually a brighter green than the leading edges, which consisted of tightly clustered arrays of cells protruding from the microcolony that occasionally extended towards other microcolonies or the microcolony from which it emerged (Fig. 1B to D, L, M, and O).

Dynamics of microcolony development by nonfilamented cells in the PEG 200-, NaCl-, and −0.25-MPa-water-potential PEG 8000-treated samples were similar to those of the unamended samples, except that there were fewer growth projections away from the colony center, and those that did form were shorter, rounder, and rarely made contact with neighboring microcolonies (Fig. 1M). At water potentials lower than −0.25 MPa in the PEG 8000-treated samples, microcolonies were no longer elongated, but instead there was a more uniform radial expansion from the colony center (Fig. 1F to J). Occasionally, circular, rather than rod-shaped, bright green fluorescent cells were visible in the center of a colony (Fig. 1H). Microcolonies derived from filamented cells in the NaCl-treated samples did not have protrusions extending from the colony, but instead the filamented cells were tightly wrapped around and over themselves in a cluster (Fig. 1N). The rate of colony expansion was reflected by cell doubling times and length. Microcolony surface areas in the ionic- and nonionic-solute-treated samples were comparable to those in the unamended samples after 4 days yet substantially smaller in the PEG 8000-treated samples (Table 1 and data not shown).

Maturation phase. The maturation phase begins 9 to 12 h into microcolony formation when the colonies assume a more complex, three-dimensional organization. A highly organized pattern of circular cells packed in an orderly array was observed in the *x-y* sections from the top of the microcolony to the surface of the substratum in the unamended samples (Fig. 2A). This pattern was consistently observed in all sections except at the periphery of the microcolony. Since *P. putida* is a rod-shaped organism, the consistently circular shapes of bacterial cells throughout the depth of the biofilms on the unamended medium suggested that the rod-shaped cells were arranged perpendicular to the surface. In the center of the microcolonies, cell density was generally the same at all depths (Table 1). Approximately 22% of the biofilm volume contained calcofluor-stained extracellular carbohydrates (Table 1). Cells at the edges were generally arranged parallel to the surface, as was observed during early periods of microcolony development (Fig. 1C).

In the −1.5-MPa water potential, NaCl-treated sample there was a mixture of circular and oval cells (Fig. 2B) at a much lower density than in the unamended treatment (Table 1). We occasionally observed filamented cells that snaked their way through several sagital sections (data not shown). The presence of a mixture of filamented and typical rod-shaped cells suggests that some of the filamented cells were capable of fragmentation by septation during microcolony maturation. This fragmentation produces a population of ordinary-sized and filamented cells, which may explain the less orderly cell arrangement (Fig. 2A and B). In the −1.5-MPa water potential, PEG 8000-treated samples, heterogeneously distributed aggregates of small, circular cells were frequently adjacent to large regions devoid of cells (Fig. 2C), resulting in a lower cell

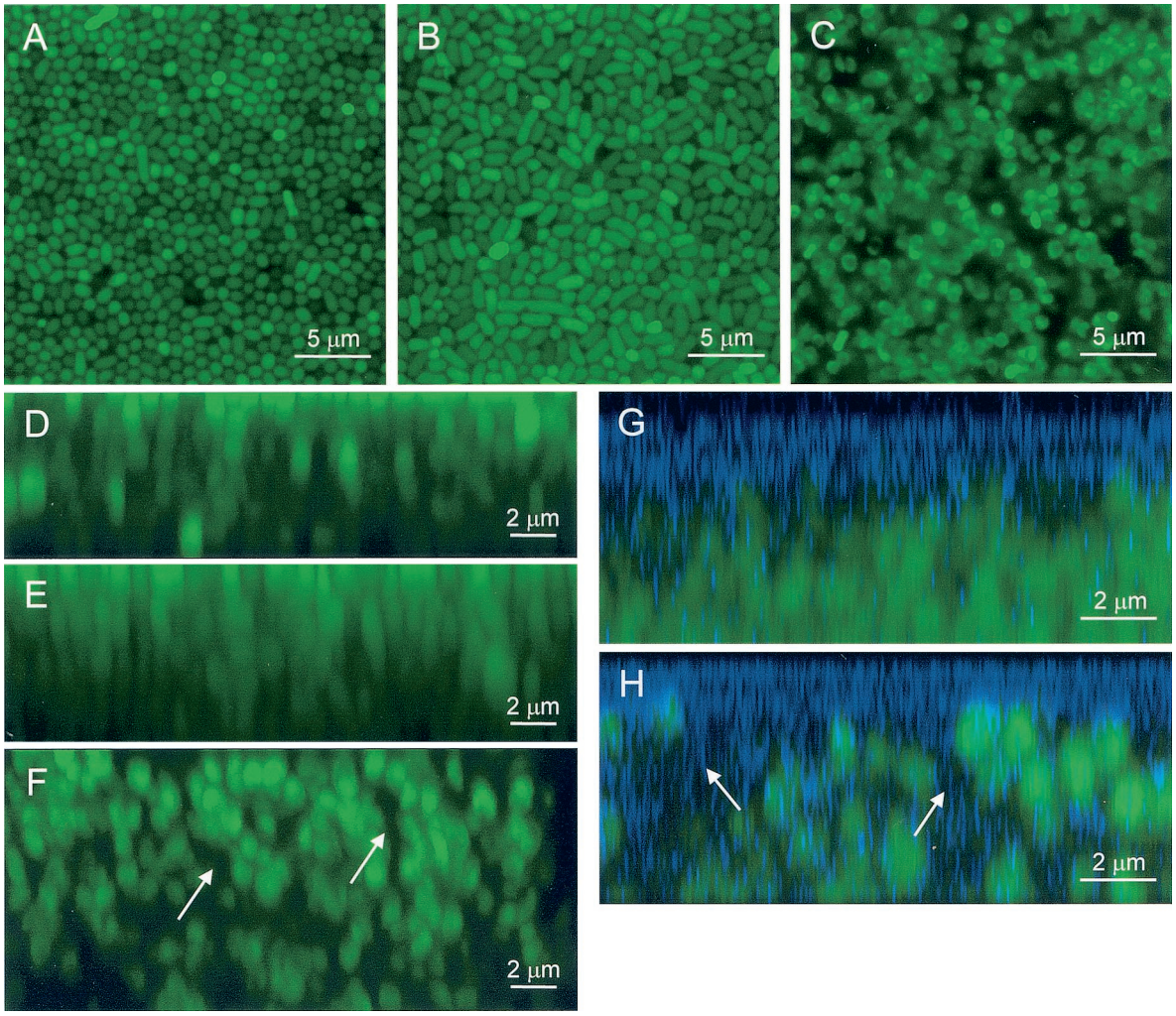

FIG. 2. Overhead (*x-y*) and sagital (*x-z*) CSLM images of 24-h-old *P. putida* mt-2 biofilms. (A, D, and G) Unamended medium; (B and E) −1.5-MPa water potential, NaCl-treated samples; (C, F, and H) −1.5-MPa water potential, PEG 8000-treated samples. Arrows indicate contiguous cell-free regions (F) containing calcofluor-stained material (H). Sagital images (*x-z*) were created from a collection of 148 (D), 160 (E), 234 (F), and 14 (G and H) overhead images with a 0.05-μm (D to F) or 0.5-μm (G, H) interval between images and were assembled with Image J software (http://rsb.info.nih.gov/nih-image). Multiple images were overlaid and cropped using Adobe Photoshop (Adobe Systems, Mountain View, Calif.).

density and a greater porosity (more cell-free areas) than in the unamended and −1.5-MPa water potential, NaCl-treated samples (Table 1).

Cell organization in the *x-z* plane shows that cells were generally arranged perpendicular to the surface in a columnar fashion throughout the depth of the microcolony (Fig. 2D to F). This change in cell orientation may occur in response to physical crowding or by surface appendages like polar type IV pili that mediate twitching motility (20). Once oriented vertically, cell growth and reproduction can proceed, which may explain our observation that cells were stacked pole to pole, two or more cells high almost directly on top of each other (Fig. 2D and E). Microcolony heights were comparable in the unamended and −1.5-MPa water potential, NaCl-treated samples and did not change over time but increased over time in the −1.5-MPa water potential, PEG 8000-treated samples (Table 1), resulting in stacks of six to nine cells in a column (Fig. 2F). In the −1.5-MPa water potential, PEG 8000-treated sample, cell-free regions of only one or two cell diameters in width containing EPS (Fig. 2F and H) spanned the height of the microcolony. The more heterogeneous distribution of cells in the −1.5-MPa water potential, PEG 8000-treated samples may create chemical gradients due to the greater tortuosity of diffusional paths around the cells, and such gradients may alter biofilm properties.

Similar arrangements of cells have been observed in colonies of various bacterial species grown on agar (9, 28) as well as in aquatic biofilms formed in flowthrough systems (6, 16). The similarity in microcolony architecture in unsaturated and saturated flowthrough biofilm systems formed by various bacterial species suggests that this pattern may be a general phenomenon reflecting growth and fitness advantages to social interactions. In other studies, cells at the bottom of unsaturated *Pseudomonas* biofilms were observed to be parallel rather than perpendicular to the membrane surface (1, 33), and this difference may have resulted from cultivating biofilms on a nylon

membrane or from the manner in which they were prepared for atomic-force microscopy.

EPS localization. Most of the calcofluor-stained material (Fig. 2G and H) was localized at the biofilm-air interface, and EPS thickness was highly variable within a treatment and greatest in the −1.5-MPa water potential, PEG 8000-treated sample (Table 1), although it generally comprised roughly only 20% of the total biofilm height in any treatment. We observed increased EPS production in response to cellular dehydration imposed by the PEG 8000 treatment, but not in response to increases in osmolarity (unpublished data). EPS viscosity is likely greater in the −1.5-MPa water potential, PEG 8000-treated sample than in the unamended samples due to the combined effect of increased EPS production, reduced water content, and reduced microcolony biovolume. Although the chemical composition of the calcofluor-stained EPS produced by *P. putida* mt-2 is unknown, the genomic sequence of *P. putida* KT2440 has revealed a novel EPS biosynthetic operon, a nearly complete alginate biosynthetic pathway, and a possible cellulose biosynthesis operon (20). Our unpublished findings demonstrate that *P. putida* mt-2 produces a uronic acid-containing EPS, presumably alginate, in the PEG 8000-treated samples with a water potential lower than −0.5 MPa, although it is clear that it is not the only, or the primary, EPS synthesized. For some bacterial species, EPS production is required for surface attachment and for the characteristic biofilm architecture in saturated systems (6, 22, 23, 35), and its overproduction can lead to altered microcolony development and biofilm properties (13). The role, if any, of these EPSs in unsaturated biofilm formation or maintenance needs to be explored more completely.

Summary. The extent to which bacteria colonize soil or plant surfaces as biofilm communities rather than as individuals is not well understood, but several reports have demonstrated the presence of biofilms in natural habitats (10, 19) and particularly on roots grown in soil containing introduced bacteria (2, 4, 26). Biofilms isolated from leaf surfaces may be tens of micrometers thick, have a copious exopolymeric matrix, form extensive networks several millimeters long, and contain several thousand or more cells (19). In this study, microcolonies in the unamended treatment were typically 175- to 250-μm across, 6-μm thick, and contained 9.4×10^4 to 1.5×10^5 cells per microcolony, assuming a density of 115 cells/100 μm^2 and a thickness of two to three cell layers, which are comparable to the densities and thicknesses of larger biofilms isolated from leaf surfaces (10, 19). The conditions that we used may not have been optimal for the synthesis of an exopolymeric matrix that is copious or complex enough to reflect those found in nature.

Bacterial biofilm formation under unsaturated conditions is a multistage process that is influenced by the availability of water. Reduced water availability affects cell growth morphologies, growth rates, and cellular physiology, all of which influence biofilm development and properties. Further studies should examine biofilm development by other organisms under conditions more accurately reflecting in situ conditions to reveal the true nature of this growth form in unsaturated habitats. The studies described here form the basis for investigations into the molecular mechanisms (surface structures, motility, and cell-cell interactions) of unsaturated biofilm biology, which is necessary for better understanding bacterial ecology in terrestrial habitats.

We thank Margie Carter for technical assistance with the confocal microscopy.

This research was supported by grants from the Mary and Raymond Baker Family Trust, the Agronomy Department of Iowa State University, and the Iowa Agriculture and Home Economics Experiment Station.

REFERENCES

1. **Auerbach, I. D., C. Sorensen, H. G. Hansma, and P. A. Holden.** 2000. Physical morphology and surface properties of unsaturated *Pseudomonas putida* biofilms. J. Bacteriol. **182:**3809–3815.
2. **Bloemberg, G. V., A. H. Wijfjes, G. E. Lamers, N. Stuurman, and B. J. Lugtenberg.** 2000. Simultaneous imaging of *Pseudomonas fluorescens* WCS365 populations expressing three different autofluorescent proteins in the rhizosphere: new perspectives for studying microbial communities. Mol. Plant-Microbe Interact. **13:**1170–1176.
3. **Chandra, J., D. M. Kuhn, P. K. Mukherjee, L. L. Hoyer, T. McCormick, and M. A. Ghannoum.** 2001. Biofilm formation by the fungal pathogen *Candida albicans*: development, architecture, and drug resistance. J. Bacteriol. **183:** 5385–5394.
4. **Chin-A-Woeng, T. F. C., W. de Priester, A. J. van der Bij, and B. J. J. Lugtenberg.** 1997. Description of the colonization of a gnotobiotic tomato rhizosphere by *Pseudomonas fluorescens* biocontrol strain WCS365, using scanning electron microscopy. Mol. Plant-Microbe Interact. **10:**79–86.
5. **Costerton, J. W., Z. Lewandowski, D. E. Caldwell, D. R. Korber, and H. M. Lappin-Scott.** 1995. Microbial biofilms. Annu. Rev. Microbiol. **49:**711–745.
6. **Danese, P. N., L. A. Pratt, and R. Kolter.** 2000. Exopolysaccharide production is required for development of *Escherichia coli* K-12 biofilm architecture. J. Bacteriol. **182:**3593–3596.
7. **Davey, M. E., and G. A. O'Toole.** 2000. Microbial biofilms: from ecology to molecular genetics. Microbiol. Mol. Biol. Rev. **64:**847–867.
8. **Davies, D. G., M. R. Parsek, J. P. Pearson, B. H. Iglewski, J. W. Costerton, and E. P. Greenberg.** 1998. The involvement of cell-to-cell signals in the development of a bacterial biofilm. Science **12:**299–312.
9. **Enos-Berlage, J. L., and L. L. McCarter.** 2000. Relation of capsular polysaccharide production and colonial cell organization to colony morphology in *Vibrio parahaemolyticus.* J. Bacteriol. **182:**5513–5520.
10. **Fett, W. F.** 2000. Naturally occurring biofilms on alfalfa and other types of sprouts. J. Food Prot. **63:**625–632.
11. **Halverson, L. J., and M. K. Firestone.** 2000. Differential effects of permeating and nonpermeating solutes on the fatty acid composition of *Pseudomonas putida.* Appl. Environ. Microbiol. **66:**2414–2421.
12. **Harris, R. F.** 1981. Effect of water potential on microbial growth and activity, p. 23–96. *In* R. F. Parr, W. F. Gardner, and L. F. Elliot (ed.), Water potential relations in soil microbiology. Soil Science Society of America, Madison, Wis.
13. **Hentzer, M., G. M. Teitzel, G. J. Balzer, A. Heydorn, S. Molin, M. Givskov, and M. R. Parsek.** 2001. Alginate overproduction affects *Pseudomonas aeruginosa* biofilm structure and function. J. Bacteriol. **183:**5395–5401.
14. **Heydorn, A., B. Ersbøll, J. Kato, M. Hentzer, M. R. Parsek, T. Tolker-Nielsen, M. Givskov, and S. Molin.** 2002. Statistical analysis of *Pseudomonas aeruginosa* biofilm development: impact of mutations in genes involved in twitching motility, cell-to-cell signaling, and stationary-phase sigma factor expression. Appl. Environ. Microbiol. **68:**2008–2017.
15. **Jensen, R. H., and C. A. Woolfolk.** 1985. Formation of filaments by *Pseudomonas putida*. Appl. Environ. Microbiol. **50:**364–372.
16. **Lawrence, J. R., D. R. Korber, B. D. Hoyle, J. W. Costerton, and D. E. Caldwell.** 1991. Optical sectioning of microbial biofilms. J. Bacteriol. **173:** 6558–6567.
17. **Mattick, K. L., F. Jørgensen, J. D. Legan, M. B. Cole, J. Porter, H. M. Lappin-Scott, and T. J. Humphrey.** 2000. Survival and filamentation of *Salmonella enterica* serovar Enteritidis PT4 and *Salmonella enterica* serovar Typhimurium DT104 at low water activity. Appl. Environ. Microbiol. **66:** 1274–1279.
18. **Miller, W. G., J. H. Leveau, and S. E. Lindow.** 2000. Improved *gfp* and *ina*Z broad-host-range promoter-probe vectors. Mol. Plant-Microbe Interact. **13:** 1243–1250.
19. **Morris, C. E., J.-M. Monier, and M.-A. Jacques.** 1997. Methods for observing microbial biofilms directly on leaf surfaces and recovering them for isolation of culturable microorganisms. Appl. Environ. Microbiol. **63:**1570–1576.
20. **Nelson, K. E., C. Weinel, I. T. Paulsen, R. J. Dodson, H. Hilbert, V. A. P. Martins dos Santos, D. E. Fouts, S. R. Gill, M. Pop, M. Holmes, L. Brinkac, M. Beanan, R. T. DeBoy, S. Daugherty, J. Kolonay, R. Madupu, W. Nelson, O. White, J. Peterson, H. Khouri, I. Hance, P. Chris Lee, E. Holtzapple, D. Scanlan, K. Tran, A. Moazzez, T. Utterback, M. Rizzo, K. Lee, D. Kosack, D. Moestl, H. Wedler, J. Lauber, D. Stjepandic, J. Hoheisel, M. Straetz, S.**

Heim, C. Kiewitz, J. A. Eisen, K. N. Timmis, A. Düsterhöft, B. Tümmler, and C. M. Fraser. 2002. Complete genome sequence and comparative analysis of the metabolically versatile *Pseudomonas putida* KT2440. Environ. Microbiol. **4:**799–808.

21. **Newman, D. L., and J. A. Shapiro.** 1999. Differential *fiu-lacZ* fusion regulation linked to *Escherichia coli* colony development. Mol. Microbiol. **33:**18–32.
22. **Nivens, D. E., D. E. Ohman, J. Williams, and M. J. Franklin.** 2001. Role of alginate and its O acetylation in formation of *Pseudomonas aeruginosa* microcolonies and biofilms. J. Bacteriol. **183:**1047–1057.
23. **O'Toole, G., H. B. Kaplan, and R. Kolter.** 2000. Biofilm formation as microbial development. Annu. Rev. Microbiol. **54:**49–79.
24. **Papendick, R. I., and G. S. Campbell.** 1980. Theory and measurement of water potential, p. 1–22. *In* J. F. Parr, W. R. Gardner, and L. F. Elliott (ed.), Water potential relations in soil microbiology. Soil Science Society of America, Madison, Wis.
25. **Purevdorj, B., J. W. Costerton, and P. Stoodley.** 2002. Influence of hydrodynamics and cell signaling on the structure and behavior of *Pseudomonas aeruginosa* biofilms. Appl. Environ. Microbiol. **68:**4457–4464.
26. **Ramos, C., L. Mølbak, and S. Molin.** 2000. Bacterial activity in the rhizosphere analyzed at the single-cell level by monitoring ribosome contents and synthesis rates. Appl. Environ. Microbiol. **66:**801–809.
27. **Rauprich, O., M. Matsushita, C. J. Weijer, F. Siegert, S. E. Esipov, and J. A. Shapiro.** 1996. Periodic phenomena in *Proteus mirabilis* swarm colony development. J. Bacteriol. **178:**6525–6538.
28. **Shapiro, J. A.** 1985. Scanning electron microscope study of *Pseudomonas putida* colonies. J. Bacteriol. **164:**1171–1181.
29. **Shapiro, J. A.** 1995. The significances of bacterial colony patterns. Bioessays **17:**597–607.
30. **Shapiro, J. A., and C. Hsu.** 1989. *Escherichia coli* K-12 cell-cell interactions seen by time-lapse video. J. Bacteriol. **171:**5963–5974.
31. **Shaw, M. K.** 1968. Formation of filaments and synthesis of macromolecules at temperatures below the minimum for growth of *Escherichia coli.* J. Bacteriol. **95:**221–230.
32. **Smibert, R. M., and N. R. Krieg.** 1994. Phenotypic characterization, p. 607–665. *In* P. Gerhardt et al. (ed.), Methods for general and molecular bacteriology. ASM Press, Washington, D.C.
33. **Steinberger, R. E., A. R. Allen, H. G. Hansa, and P. A. Holden.** 2002. Elongation correlates with nutrient deprivation in *Pseudomonas aeruginosa* unsaturated biofilms. Microb. Ecol. **43:**416–423.
34. **Stoodley, P., D. deBeer, and Z. Lewandowski.** 1994. Liquid flow in biofilm systems. Appl. Environ. Microbiol. **60:**2711–2716.
35. **Watnick, P. I., and R. Kolter.** 1999. Steps in the development of a *Vibrio cholerae* El Tor biofilm. Mol. Microbiol. **34:**586–595.